Talanta 115 (2013) 779–786

Contents lists available at SciVerse ScienceDirect

Talanta

journal homepage: www.elsevier.com/locate/talanta

A new electrochemical sensor for OH radicals detection

Isacco Gualandi, Domenica Tonelli*

Dipartimento di Chimica Industriale "Toso Montanari", University of Bologna, INSTM, UdR Bologna, Viale Risorgimento 4, 40136 Bologna, Italy

ARTICLE INFO

Article history:
Received 15 March 2013
Received in revised form
20 June 2013
Accepted 25 June 2013
Available online 29 June 2013

Keywords:
OH radical detection
Modified electrodes
Aromatic hydroxylation
OH production
TiO_2 nanoparticles

ABSTRACT

A new, cheap modified electrode for indirect detection of OH radical is described. A glassy carbon (GC) electrode was modified with a polyphenol film prepared by oxidative potentiostatic electropolymerization of 0.05 M phenol in 1 M H_2SO_4. The film having a thickness of ~10 nm perfectly covered the GC surface and inhibited the charge transfer of many redox species. The degradation of the polyphenol film, that was induced by OH radicals generated by Fenton reaction or by H_2O_2 photolysis, is the analytical signal and it was evaluated by cyclic voltammetry and chronoamperometry using the redox probe $Ru(NH_3)_6^{3+}$. Some simulations of the kinetics of the reactions occurring in the solution bulk and near the electrode surface were carried out to fully understand the processes that lead to the analytical signal. The modified electrode was used to evaluate the performances of different TiO_2-based photocatalysts and the results were successfully compared with those obtained from a traditional HPLC method that is based on the determination of the hydroxylation products of salicylic acid.

1. Introduction

Free radicals, like hydroxyl (OH) and superoxide (O_2^-), are among the most reactive species that are known. When the radical production is higher than the cellular antioxidant defense, some radical chain reactions may take place with consequent attack to a lot of biological macromolecules leading to cellular damage and thus inducing many diseases, such as ischemia/reperfusion injury [1], hepatitis [2], Parkinson's and Alzheimer's diseases [3–5], rheumatoid arthritis [6], brain ischemia [7], stroke [8] and carcinogenesis [9]. The strongly oxidant capacity of OH radical, which can be produced by the Fenton reaction [10], simple ozonation [11], sonolysis [12] and other similar processes [13,14], is used to mineralize aqueous organic species. Moreover, the OH radical plays an important role in the environmental chemistry for the degradation of persistent pollutants, especially in atmosphere [15,16]. Due to its involvement in fields of outstanding interest, a simple, selective and fast determination of OH is very important.

The very high reactivity of OH radical is responsible for its very short half-life (about 10^{-10} s) [17] which explains why its concentration is generally very low. The direct determination of the OH radical is quite difficult for some matrices. For example the in vivo measurement by electron paramagnetic resonance (EPR) fails because the presence of scavengers leads to an extremely low steady-state concentration. The simplest way to detect OH radicals is indirect, i.e. by using a probe which reacts very quickly with them. Aromatic compounds, such as salicylic acid and phenylalanine, are widely used to this aim, since their reactions with OH radicals, termed aromatic hydroxylations, display very high kinetic constants [17]. The quantitative determination is performed following either the degradation of the probe or the formation of characteristic products that can be easily detected with a lot of analytical techniques like EPR [18,19], high performance liquid chromatography with electrochemical detection (HPLC-ED) [20,21], capillary electrophoresis (EC) [22], gas chromatography/mass spectrometry (GC–MS) [23], chemiluminescence [24], and micellar electrokinetic capillary chromatography (MECC) [25]. The concentration of a characteristic product is expressed by the following equation:

$$[\text{probe product}] = [\text{OH}] \cdot \eta \cdot k_p \cdot [\text{probe}]/(k_p \cdot [\text{probe}] + k_m \cdot [matrix]) \quad (1)$$

Where [*OH*] is the OH concentration in the sample, η is the yield of the reaction between the radical and the probe to form the detected product, k_p is the kinetic constant of the same reaction, [probe] is the probe concentration, and $k_m \cdot [matrix]$ is the term that evaluates the OH radicals that react with the matrix. For most matrices this term is numerically unknown and comparable to the probe term; therefore a rigorous quantification of the OH concentration is extremely difficult. However, it is possible to make a relative scale of ·OH production/concentration when analyzing a single matrix at different conditions or similar matrices [26].

Electrochemical methods are a tool that can ensure a rapid and direct quantification of both the probe and its reaction products with the OH radical [17], but the presence of a lot of reducible or

* Corresponding author. Tel.: +39 0 51 209 3667; fax: +39 0 51 209 36 90.
E-mail address: domenica.tonelli@unibo.it (D. Tonelli).

0039-9140/$ - see front matter © 2013 Elsevier B.V. All rights reserved.
http://dx.doi.org/10.1016/j.talanta.2013.06.043

oxidizable substances in real samples could be a limit for a large application. A simple electroanalytical approach, based on the attack of chemically modified electrodes (CMEs) by oxygen radicals, has been recently proposed in some papers [27–29] where DNA or a self-assembled monolayer of alkylthiol was used as the electrode modifier. The modified electrode was dipped in a solution where OH radicals were generated. After exposing the electrode to the radical attack the amount of modifier destroyed by the OH radicals was evaluated. Therefore, the electrode modifier can effectively operate as a probe and no chromatographic or electrophoretic separations are necessary since a single electrochemical measurement on the CME is sufficient, once it has been removed from the matrix under investigation.

Herein, a modified electrode for the indirect OH radical detection is described. A phenol based polymer was chosen as the electrode modifier due to the high kinetic constant and good selectivity of the aromatic hydroxylation reaction which make it suitable and widely used for the OH radical detection.

2. Materials and method

2.1. Chemicals

L-Ascorbic, hexaamminoruthenium (III) chloride, hydrogen peroxide solution (30% w/w), 2,2'-azino-bis-(3-ethylbenzothiazolin-6-sulfonic acid) (ABTS), 2,2'-azobis-2-methyl-propanimidamide dihydrochloride (AAPH) were bought from Sigma-Aldrich. Sodium acetate, ferrous sulfate, phenol, sodium persulfate and sodium carbonate were purchased from Carlo Erba. Acetic acid, potassium permanganate and acetonitrile were purchased from Baker.

2.2. Instrumentation

All the electrochemical experiments were carried out in a single compartment three-electrode cell. All potentials were measured with respect to an aqueous saturated calomel electrode (SCE). A Pt wire was used as the counter electrode. A 3 mm glassy carbon (GC) purchased from Metrohm was used as the working electrode. The experiments were carried out using a CHInstruments Mod. 660C, controlled by a personal computer via CHInstruments software.

2.3. Electrode modification

Prior to each experiment, the GC electrode was cleaned first with sand-paper and then with aqueous alumina (0.05 μm) slurry on a wet polishing cloth to remove all residues of old films and to regenerate the mirror surface. Then the $Ru(NH_3)_6^{3+}$ signal was recorded by chronoamperometry (CA) or cyclic voltammetry (CV) as described below. The electropolymerization of phenol was carried out by applying a potential of+1.0 V to the GC electrode soaked in a solution containing 0.05 M phenol in 1 M sulfuric acid, for 60 s. Then the film was stabilized by five cycles of potential between 0 and +0.8 V. To make sure a successful deposition of a well-adhered polyphenol film had been accomplished, a CV (in 50 mM acetate buffer, pH 4.6, containing 5 mM $Ru(NH_3)_6^{3+}$) was recorded. The absence of the $Ru(NH_3)_6^{3+}$ signal in the cyclic voltammogram indicated a satisfactory deposition and led to the next experimental steps. Differently, if the $Ru(NH_3)_6^{3+}$ signal was observed, the film was prepared again.

The sensor was stored in the dark in 0.5 M acetate buffer pH 4.6 and it was stable for a week at least; moreover, after exposure to the OH radicals the signal remained unchanged for about 24 h. On the contrary, if the sensor was kept in air, the "blank" signal was not stable and displayed a noticeable increase probably due to a breakage of the polyphenol film in dry conditions.

2.4. Generation of OH radical

The OH radical was generated both by the Fenton reaction and by the photolysis of hydrogen peroxide.

When the Fenton reaction was used, the modified electrode was soaked in 20 mL of a 0.05 M $FeSO_4$ solution in 0.05 M acetate buffer (pH 4.6). Variable volumes of hydrogen peroxide necessary to reach concentrations between 0.1 and 0.5 M were added to the stirred solution. The stirring was stopped after 10 s. After 5 min the electrode was drawn out from the solution, washed with water and soaked in 0.5 M acetate buffer solution (pH 4.6) containing 5 mM $Ru(NH_3)_6^{3+}$. Afterwards, CV and CA responses were recorded.

To perform the photolytic generation, H_2O_2 solutions at variable concentrations (0.1–0.5 M) were put into the photolysis reactor along with the modified electrode which was placed as near as possible to the lamp. Then the lamp operating at 254 nm (UV 18 F, Italquarz, with emission power of 17 W) was switched on. After the irradiation, the electrode was taken out from the reactor, rinsed with doubly distilled water and the CV and CA signals related to $Ru(NH_3)_6^{3+}$ redox system were recorded.

2.5. Quantification of the film degradation by ·OH attack

Owing to their high reactivity, the OH radicals coming in contact with the polyphenol film can attack the polymer causing its degradation. As a result, this reaction leaves the GC surface partially uncovered. As shown in Fig. 3, although the polyphenol has an insulating behavior, its degradation restores the conductive character of the underlying GC electrode. Therefore, the OH concentration can be determined estimating the extent of the polymeric film degradation. This was quantified by means of the redox probe $Ru(NH_3)_6^{3+}$ whose electrochemical behavior at the modified electrode was investigated by CV and CA. The cyclic voltammetry was recorded between 0 and −0.7 V at 0.05 V s^{-1} and the percentage of degraded polyphenol, D_{CV} (%), was evaluated through Eq. (2), as reported by Scholtz et al. [28] when evaluating the degradation degree of an insulating self-assembled monolayer of alkanethiols

$$D_{CV}(\%) = I_f \cdot 100/I_{GC} \quad (2)$$

Where I_f is the anodic peak current recorded at the modified electrode for the $Ru(NH_3)_6^{3+}/Ru(NH_3)_6^{2+}$ couple after partial degradation of the polymer film and I_{GC} is the anodic peak current recorded at a bare GC electrode. The minimum signal that could be measured by CV corresponded to an uncovered area of 2%, but more precise values of I_f were obtained for percentages higher than 5%. The upper limit of the linear response was calculated studying the degradation kinetics of the polyphenol film when the OH radical was generated by 0.5 M H_2O_2 photolysis. D_{CV} (%) was directly proportional to time and, therefore, to the amount of the radicals reaching the electrode, until 70% uncovered area (see Fig. B1 in SI). Therefore, the useful range of CV method is 2–70%.

Chronoamperometry (initial potential: −0.1 V; quiet time: 30 s; step pulse: negative down to −0.3 V; number of step: 1; pulse width: 30 s; sample interval: 0.0005 s) was carried out in the same solution used for CV. The evaluation of the uncovered electrode area is based on the pinhole model [30,31] that was developed to calculate the current flowing through a surface covered by an insulating film which displays equally distributed holes. The current at such electrode, $i(t)$, normalized by the current, $i_d(t)$, recorded at the bare electrode at the same times

since pulse application, is given by

$$i(t)/i_d(t) = (1/\sigma^2 - 1) \cdot \{\sigma \cdot e^{-\tau} - 1 + \sigma^2(\pi \cdot T)^{1/2} \cdot e^{T} \cdot [\mathrm{erf}(\sigma \cdot T^{1/2}) - \mathrm{erf}(T^{1/2})]\} \quad (3)$$

Where θ is the fractional coverage of the electrode surface, $\sigma = \theta/(1-\theta)$, $T = \tau/(\sigma^2 - 1)$, $\tau = l \times t$, and l is a function of the diffusion coefficient D, the hole size and distribution and θ. Note that at short times (small t values), when the diffusion layer is much smaller than the hole dimensions, the current ratio reaches the value of $1-\theta$, since the redox reaction of the probe occurs directly on the electrode surface only within the pores of the film. At long times, when the thickness of the diffusion layer is large in comparison with the size of the holes, the ratio is close to one. In this case the diffusion layers from the individual sites overlap and merge so that the modified electrode behavior approaches that of the bare electrode.

The film degradation can be evaluated plotting the ratio $i(t)/i_d(t)$ versus log time. In fact, as already discussed, at short times the ordinate value is constant and equal to $1-\theta$, i.e. the percentage of the uncovered surface after the radical attack. The validity of the pinhole model for the electrode modified with the polyphenol film after partial degradation was checked by plotting the experimental ratios $i(t)/i_d(t)$ versus log time since all the variables, appearing in Eq. (3), cannot be determined. To this aim, a chronoamperogram of the redox probe was recorded with the bare electrode, then the same electrode was modified with the polyphenol film and after submission to the attack of the Fenton-generated OH radicals, an additional chronoamperogram was run. The plot obtained for our electrode (Fig. 1) shows the typical shape reported in the literature, hence it could be assumed that the chosen model is satisfactory.

The greatest percentage of the uncovered area that could be determined by CA was related to the instability of $i(t)/i_d(t)$ graphs. The curve recorded during the degradation of the polyphenol film (OH generation mode: photolysis; $[H_2O_2] = 0.1$ M; see Fig. B2 in SI) showed that the $i(t)/i_d(t)$ curves no longer followed the expected trends if the uncovered area was higher than 45%. To estimate the minimum percentage of uncovered area detectable by CA, we have taken into account the response to $Ru(NH_3)_6^{3+}$ of five just prepared films. This "blank" signal corresponded to an average uncovered area ($\pm$ SD) of 0.2 ± 0.02%. According to the usual definition of limit of detection (LOD) and limit of quantification (LOQ), these limits for the uncovered area resulted 0.26% and 0.4%, respectively.

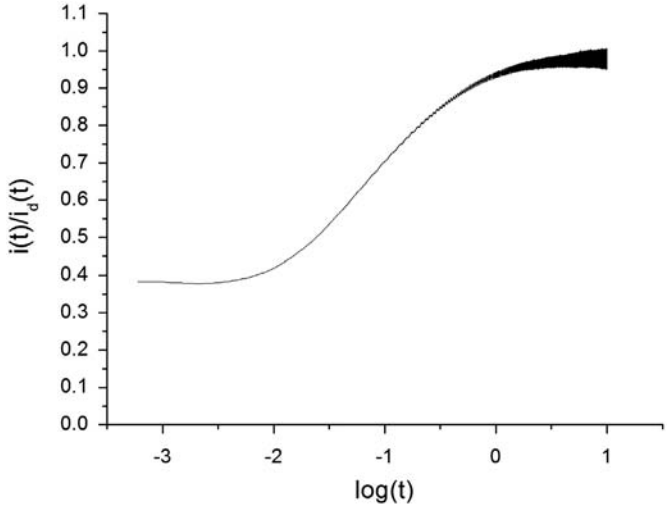

Fig. 1. Graph of $i(t)/i_d(t)$ vs. $\log(t)$ for CA experiments carried out in 0.5 M buffer acetate (pH = 4.6) containing 5 mM $Ru(NH_3)_6^{3+}$. The meanings of $i(t)$ and $i_d(t)$ have been given above (conditions of the Fenton reaction: $[Fe^{2+}] = 0.5$ M; $[H_2O_2] = 0.5$ M; time = 5 min). The constant value at short times is equal to $1-\theta$.

Therefore, the determination of the uncovered GC surface by CA is more correct than by CV when the extent of degradation is little since the capacitive current makes it difficult to evaluate the anodic peak current by CV. On the contrary, when the polyphenol film is highly degraded, CV was preferred as the graph $i(t)/i_d(t)$ versus log time does not have a definite shape, probably due to the fact that the holes in the film merge together making the model no longer acceptable. On the other hand, from the values reported above for CV and CA, we can state that both techniques can be employed in the range 2–45%.

2.6. Evaluation of photocatalyst activity of TiO_2 nanoparticles

The OH produced by five different photocatalysts based on TiO_2 nanoparticles was analyzed both using the proposed method and a more traditional OH trapping method that exploits salicylic acid (SA) as the ·OH probe. The GC electrode modified by the polyphenol film was soaked in a suspension of 3% (w/w) TiO_2 nanoparticles which was irradiated for 30 min by a Radium lamp (Radium, Sanolux, HRC 300-280, power: 300 W), which replicates the solar spectrum. Then the electrode was taken out of the solution, washed and used to evaluate via CA the charge exchanged by the $Ru(NH_3)_6^{3+}/Ru(NH_3)_6^{2+}$ couple.

A 0.3% (w/w) suspension of TiO_2 nanoparticles containing 4×10^{-4} M SA was irradiated for 30 min. The SA hydroxylation was followed by HPLC via fluorimetric detection ($\lambda_{exc} = 320$ nm; $\lambda_{em} = 440$ nm) analyzing a small aliquot (1 mL) of the suspension after 5, 15, and 30 min of irradiation. Then the sample was diluted 1:50 with 0.1 M phosphate buffer solution (pH 7.0) to induce the TiO_2 nanoparticles coagulation. The sample was filtered through a nylon filter (pore size 0.45 μm) and injected into the liquid chromatograph, using a 200 μL loop. The mobile phase consisted of a 10 mM phosphate buffer (pH 6.0) containing 0.02% (w/v) sodium azide. The chromatogram showed a good separation between the peaks of SA, 2,3-dyhydroxy benzoic acid (2,3-DBHA) and 2,5-dyhydroxy benzoic acid (2,5-DBHA) which are formed by the reaction between the OH radicals and SA. Since 2,5-DBHA has a higher response factor than 2,3-DBHA (about 20 times), it was used as the probe product to be inserted in Eq. (1). The rate of ·OH production was evaluated only from the data relevant to 5 min irradiation, because longer times led to 2,5-DBHA concentrations which were of the same order of magnitude as SA concentration. In such conditions, the 2,5-DBHA consumption due to the reaction with the OH radicals is also significant, since the kinetic constants of the reactions of ·OH with SA and 2,5-DBHA are similar. Consequently, the OH production rate that was estimated by 2,5-DBHA concentration at time longer than 5 mim would be underestimated.

3. Results

3.1. Optimization of the polyphenol deposition

The electrochemical oxidation of phenol leads to the formation of phenoxy radicals which can couple to form a dimer. These dimers can themselves be oxidized and further react with the phenoxy radicals or other dimeric radicals to produce higher molecular weight material. The polyphenol is characterized by low oxidation rates, low permeability, and strong adhesion to the GC surface [32,33].

In order to find the best operative parameters for our purposes, three different methods for the electrochemical synthesis of polyphenol were tested.

In particular, on the basis of the results obtained by Gattrel and Kirk [33], a film (F1) was prepared from a 0.05 M phenol solution in aqueous 1 M H_2SO_4 by applying a potential of +1.0 V for 60 s. As shown by Gattrel et al. [33] this kind of preparation leads to a polymer where all the monomeric units are linked by C–C bonds. In theory, such a structural feature can increment the susceptibility of the phenol rings towards the OH radicals attack. Another film (F2) was prepared from a basic solution using cyclic voltammetry [34]. The GC electrode was cycled five times between –1.0 and +1.3 V in 0.1 Na_2CO_3 solution containing 0.05 M phenol. In this case, the resulting polymer should exhibit ether linkages between the aromatic rings. The third film (F3) was electrosynthesized in conditions similar to those employed for F1 except for the substitution of aqueous sulfuric acid with acetonitrile. Moreover, the synthesis was carried out under nitrogen atmosphere in order to remove any source of oxygen which could introduce further oxidized functionalities on the benzene rings.

Two different series of experiments were carried out on the three films to assess their insulating behavior and their reactivity towards the OH radicals. Clearly, the best candidate for our analytical purpose will have to display the greatest insulating properties as well as the highest reactivity toward the OH radicals.

The insulating behavior with respect to the electron-transfer of $Ru(NH_3)_6^{3+}/Ru(NH_3)_6^{2+}$ couple was verified by both CV and CA on the freshly prepared electrodes and the recorded response represents the blank signal for the modified GC electrode.

As expected, F1 and F2 showed an insulating behavior when characterized by CV (see Fig. 3) and CA. Differently, F3 showed the characteristic current peaks of the probe when performing cyclic voltammetry, in addition to a current significantly different from the background recorded by chronoamperometry. Probably, since the acetonitrile is a better solvent than water for polyphenol [33], the polymeric film was partly solubilized in acetonitrile, leading to some uncovered areas on the electrode surface. For this reason, F3 was discarded. In the second test the polymeric films, F1 and F2 were submitted to the attack of the Fenton-generated OH radicals ($[Fe^{++}]=0.05$ M; $[H_2O_2]=0.5$ M; [buffer acetate, pH 4.6]=0.05 M) and the percentage of degraded polyphenol was evaluated by Eqs. (2) and (3) in order to verify whether these films could be used satisfactorily for the OH radicals determination with the proposed approach. The degradation of the F1 was reproducible, and the percentage of uncovered area was equal to 22% while the F2 did not appear to be degraded since no $Ru(NH_3)_6^{3+}/Ru(NH_3)_6^{2+}$ signal was recorded after the OH radical attack. This result can be explained on the basis of the greater thickness of F2 film [33,34] and of its low reactivity due to the presence of ether linkages between the aromatic rings [32]. Following the preliminary tests which have just been described, the film F1 was selected as the most suitable for the detection of the OH radicals.

The film F1 was characterized by infrared spectroscopy (IR) and by atomic force microscopy (AFM). The IR spectrum (Fig. 2A) was compared with literature data [32]. The observed band at 1261 cm^{-1} is due to the stretching of aromatic C=C double bounds. The bands at 2957, 2924, 2854 and 1463 cm^{-1} are explainable by the presence of quinonic subunits and are related to C–H stretching (2957, 2924, and 2854 cm^{-1}) and to C=C stretching. The bands at 3417 and 1362 cm^{-1} are due to O–H and (C=C)–OH stretching, respectively. Lastly, the band recorded at 1732 cm^{-1} is due to C=O stretching. These results suggest that the film is partially oxidized (quinonic bands) and the aromatic units are essentially coupled through C–C bonds as opposed to ether linkages, since the IR spectrum confirms the signals of the OH group and of its oxidized forms.

AFM images for both, the bare GC electrode and the polyphenol-modified electrode, were recorded. The two images are very similar suggesting that the film perfectly adhered to the electrode surface and, as a consequence, its morphology adapted to the underlying surface. Moreover, a partial modification of the GC electrode was carried out to acquire an image of the boundary zone between the bare GC and modified surface (Fig. 2B). This also allowed an estimation of the thickness of the film which resulted 10 ± 1 nm.

3.2. The experimental analytical signal

A stabilized ·OH solution is not commercially available, thus, in order to evaluate the trend of the analytical signal vs. the ·OH concentration, the radical species must be produced directly in the solution where the electrode is soaked. The OH radicals were generated by Fenton reaction and H_2O_2 photolysis. Since there is no direct and simple relationship between the OH radical concentration and the composition of the solutions used for the radical generation, at first, a semi-quantitative approach had to be used to demonstrate that when the OH radicals production increases, an inherent increase of the analytical signal is also recorded. Later a more quantitative approach was utilized to

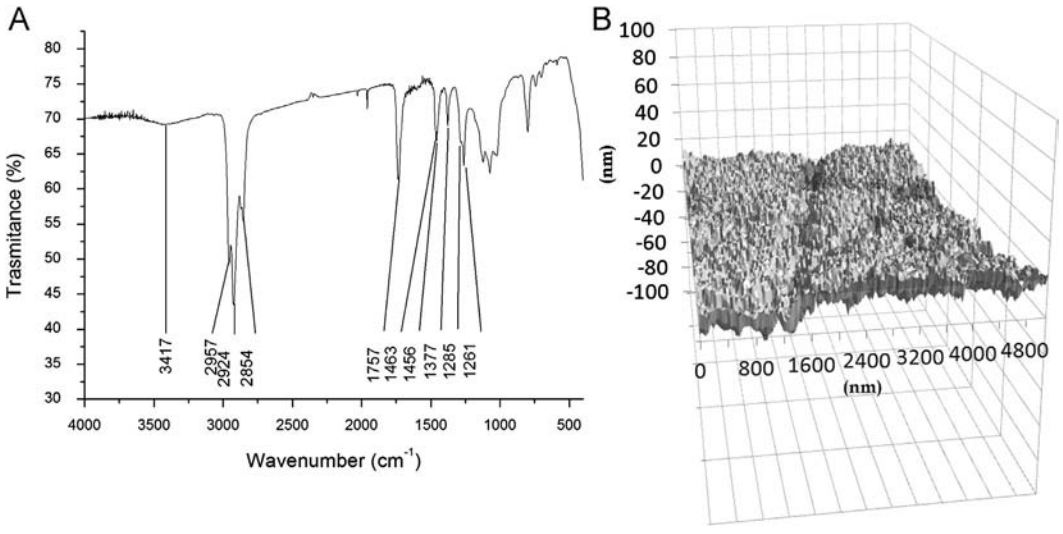

Fig. 2. IR spectrum (A) recorded with a KBr pellet containing ~2% (w/w) polyphenol electrosynthesized on a GC rod. The polymer was dissolved in acetonitrile and then dried under vacuum. AFM image (B) of the boundary zone between the bare and polyphenol-modified GC.

explain the processes and reactions from which the analytical signal originates.

The most used method to prepare the OH radicals is the Fenton reaction where Fe^{2+} reacts with H_2O_2 to form Fe^{3+}, OH^- and the OH radical. Furthermore, the OH radical can react with H_2O_2 and Fe^{2+} to yield O_2^- and Fe^{3+}, respectively. The most important reactions which control the ·OH concentration are listed below. Moreover, it is worth to notice that the OH radicals can also undergo a side-reaction with the acetate ions deriving from the buffer solution used:

Reaction (1) $Fe^{2+}+H_2O_2 \rightarrow Fe^{3+}+ \cdot OH+OH^-$
Reaction (2) $Fe^{2+}+ \cdot OH \rightarrow Fe^{3+}+OH^-$
Reaction (3) $\cdot OH+H_2O_2 \rightarrow HO_2+H_2O$
Reaction (4) $\cdot OH+ \cdot OH \rightarrow H_2O_2$
Reaction (5) $HO_2+Fe^{3+} \rightarrow Fe^{2+}+O_2+H^+$
Reaction (6) $H_2O_2+Fe^{3+} \rightarrow HO_2+Fe^{2+}+H^+$

After having kept the modified electrode in the solution where the Fenton reaction occurred for the desired time, the degradation of the polyphenol film was evaluated by CV and CA.

In Fig. 3 the effect of the electrode modification and of OH attack on the CV response of the $Ru(NH_3)_6^{3+}$/ $Ru(NH_3)_6^{2+}$ couple can be seen. On the bare GC the charge transfer is very fast and the reversible peaks system is very evident. After the modification of the electrode surface, the charge transfer becomes very slow and an insulating behavior can be observed, as indicated by the disappearance of the redox response. If the modified GC is kept in a solution where a big amount of OH radicals has been generated by the Fenton reaction, the $Ru(NH_3)_6^{3+}$/$Ru(NH_3)_6^{2+}$ peaks are almost fully restored. Control experiments were carried out to verify if hydrogen peroxide, iron(II) or iron(III) ions could attack the polyphenol film. It was demonstrated that none of these species altered the film modifying the GC surface.

Among the parameters affecting the Fenton reaction, only the H_2O_2 concentration was investigated in the range 0.1–0.4 M keeping both, the Fe^{++} concentration (0.05 M) and the pH (4.6) constant. As already described in the Experimental section, the degradations of the polyphenol films were studied by CV and CA. In both cases the uncovered area was proportional to the H_2O_2 concentration showing that the increase in the ·OH production leads to an increase in the analytical signal (see Fig. B3 in SI). This result confirms that the OH radical attack to the polyphenol film can be used to determine the OH radical concentration. However, the reproducibility of the Fenton reaction did not prove particularly high due to the limited repeatability of the mixing process during the addition of hydrogen peroxide under magnetic stirring. An efficient and highly repeatable mixing is essential to ensure that a constant number of OH radicals reach the electrode surface, especially within the first few seconds from the start of the reaction, when the ·OH production is very fast as Fe^{++} is in strong excess. As a result, the variation coefficient (CV%) associated with the polyphenol degradation process caused by the Fenton-generated OH radicals, expressed in terms of percentage of degraded film, was ~30%. Therefore, the OH radical generation was also attempted by hydrogen peroxide photolysis with a H_2O_2 concentration of 0.5 M and an irradiation time of 5 min. In this case, the average uncovered surface resulted 20 ± 2% (average ± standard deviation, $n=5$), indicating a higher reproducibility compared with the Fenton process (CV% =10). The reproducibility associated to the uncovered area determination was also evaluated using a lower concentration of H_2O_2 (0.01 M) for the same irradiation time, again, obtaining a CV%~10. In particular, the average percentage of the uncovered area resulted 4.9 ± 0.5% ($n=5$). For the photolysis production the film degradations were investigated at different H_2O_2 concentrations (0.01–0.5 M) for 5 min irradiation time. Also in this case a linear correlation between the uncovered area and H_2O_2 concentration was observed, in agreement with what obtained for the Fenton reaction.

In order to prove the reliability of the proposed electrochemical approach in estimating the ·OH scavenging activity of antioxidant compounds, the degradation of the film was studied in the presence of ascorbic acid (AA) at different concentrations (exposition time=10 min; generation mode: photolysis; H_2O_2=0.5 M). AA is known to react very quickly with the OH radicals causing a decrease in their concentration and, consequently, a drop of the analytical signal. As shown in Fig. 4 the degradation of the polymeric film, evaluated by CV, proceeds to a lower extent when the AA concentration is increased. For concentrations higher than 20 mM no degradation was observed during the irradiation time. This preliminary result indicates that the proposed electrode could

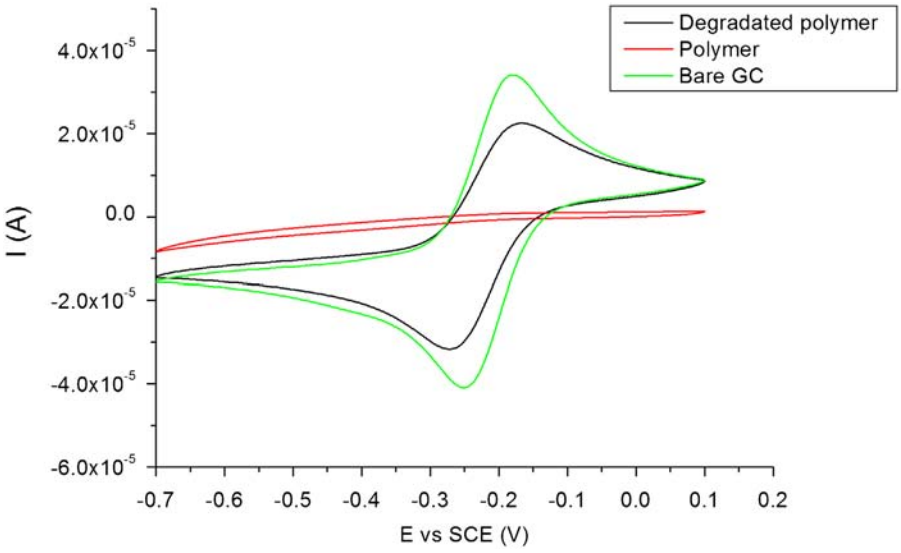

Fig. 3. CVs (scan rate: 0.05 V s^{-1}) recorded in 0.5 M acetate buffer (pH=4.6) containing 5 × 10^{-3} M $Ru(NH_3)_6^{3+}$ at bare GC, polyphenol-GC as prepared and after 5 min long attack by OH radicals (Fenton reaction conditions: [Fe^{++}] =0.5 M, [H_2O_2]=0.5 M).

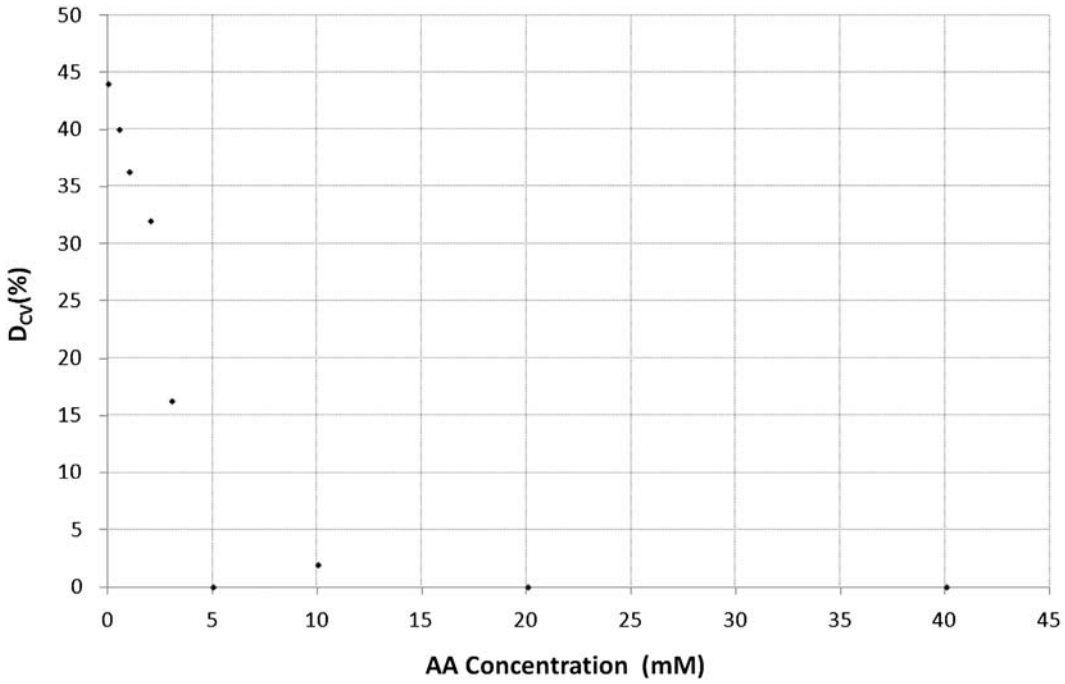

Fig. 4. Uncovered area observed for polyphenol modified electrodes that were attacked by OH radical generated by H_2O_2 photolysis ($[H_2O_2]=0.5$ M; irradiation time = 10 min) in the presence of AA different concentrations.

be satisfactorily employed for applications in different fields of interest.

3.3. Theoretical explanation of the analytical signal

Some simulations of the kinetics of the processes occurring in the solution bulk and in close proximity to the electrode surface were carried out to understand the processes and the reactions from which the analytical signal stems and to indentify the most suitable concentration range to operate.

As far as the Fenton reaction is concerned, a simulation was performed considering the reactions (1)–(6) as well as the reaction between acetate and OH radical. For all the reactions the kinetic constants were found in the literature [35] with the exception of reaction 5 for which only a range of values (0.01–0.001 $M^{-1}\,s^{-1}$) is reported [36]. Consequently, a mean value of 0.005 $M^{-1}\,s^{-1}$ was used. The differential equations deriving from the simulation are reported in the Appendix A. During the first seconds after the addition of H_2O_2 the reactions (1)–(5) are very fast and the OH radical concentration is relatively high but it quickly decreases reaching a steady state value after 5–10 s. The calculated $\cdot$OH concentrations were in the range 9×10^{-12}–5×10^{-11} M when H_2O_2 concentration was in the range 0.1–0.4 M.

As to the H_2O_2 photolysis the simulation was carried out considering a photolysis constant of $5.61\times10^{-4}\,s^{-1}$ obtained by a cross section [37] of 7.4×10^{-20} cm^2 and a quantum yield [38] of 0.5. Moreover, the reactions (3) and (4) were taken into account. The results of the simulation (see Appendix A) showed that the $\cdot$OH concentration is constant ($[OH]=4.2\times10^{-11}$ M) independently of the H_2O_2 concentration. This could be explained, on first approximation, considering that H_2O_2 is involved in reactions of both, formation and consumption of the OH radical. The $\cdot$OH concentration, finally, depends only on the kinetic constants of photolysis and reaction (3). However, the experimental results show that the H_2O_2 concentration visibly affects the analytical signal, suggesting that all the reactions determining the $\cdot$OH concentration in the solution bulk occur also in the diffusion layer near the electrode surface which originates from the very fast reaction with the polyphenol film. For this reason Fick's laws are not applicable and the $\cdot$OH concentration in the bulk of the solution is no longer proportional to its flux towards the electrode. The consequent concentration profiles of the OH radical must be also affected by all the other bulk reactions which consume and produce the radicals. To account for this, the diffusion near the electrode surface during its exposure to the OH radical was introduced for both generation systems. The $\cdot$OH diffusion coefficient value [39] used for the calculations was 2.8×10^{-5} $cm^2\,s^{-1}$. As the reaction between the film and OH radical is very fast, the $\cdot$OH concentration on the electrode surface was forced equal to 0. When the diffusive motion was introduced in the model, the simulation applied to the $\cdot$OH generation by photolysis led to the result that an increase in the H_2O_2 concentration causes an increase of the OH radicals that reach the electrode, even if their concentration in bulk of the solution remains unchanged. The calculated radical fluxes were between 1.5×10^{-11} and 10×10^{-11} mol $dm^{-2}\,s^{-1}$ (exposition time = 5 min). Fig. 5 confirms the good agreement between the data obtained from the simulations and the uncovered area percentages, independently of the $\cdot$OH generation method.

In conclusion, the observed analytical signal is due to the OH radicals which reach the electrode surface. They do not only depend on the OH concentration of the solution bulk, but also on the diffusion process and on the reactions producing and consuming OH radicals which occur near the electrode surface.

The recorded analytical signal is related to the oxidant capacity of the OH radicals diffusing *towards* a surface, i.e. to the effect of the $\cdot$OH concentration combined with the ability of the radicals to escape from the environment where they are generated. Therefore, the proposed sensor should be useful for creating a relative scale of $\cdot$OH concentration in similar matrices, analogously to the probe methods cited in the introduction.

3.4. Interferences study

A large number of aromatic compounds are successfully used as probes for the $\cdot$OH detection due to the low susceptibility to

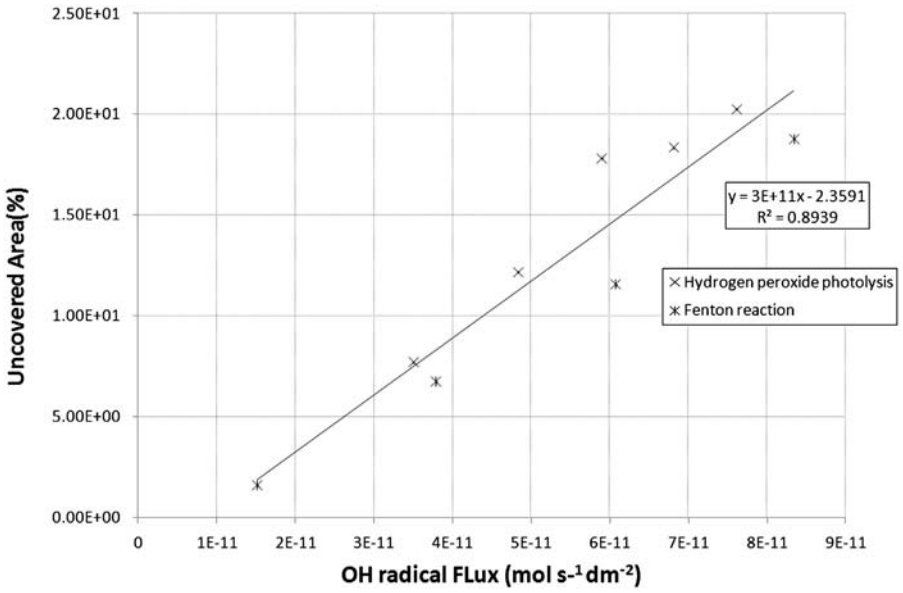

Fig. 5. Uncovered area percentage determined by CA vs. the calculated amount of OH radicals that reach the electrode surface in the different experimental setups.

interferents; therefore, the choice of an aromatic polymer, as an electrode modifier, should ensure a good selectivity. However, since this is the first time this approach is used, a study of the possible interferences was carried out.

The degradation of the insulating films of polyphenol was studied in the presence of $ABTS^{\bullet+}$ radical, alkyl peroxy radical, superoxide radical and $KMnO_4$.

The $ABTS^{\bullet+}$ solution was obtained mixing 25 μmol of ABTS with 11 μmol of $S_2O_8^{2-}$ and taking to 50 mL acetate buffer (pH 4.6) solution. The reaction requires at least 18 h to consume completely $S_2O_8^{2-}$, which is the limiting reagent. In our conditions, the final concentration of $ABTS^{\bullet+}$ radical was 4.4×10^{-4} M. The modified electrode was soaked into the solution and kept in contact with $ABTS^{\bullet+}$ radicals for 30 min. After the exposition, the $Ru(NH_3)_6^{3+}/Ru(NH_3)_6^{2+}$ signal was still absent, confirming that there is no interference from $ABTS^{\bullet+}$ radicals.

An analogous result was obtained for alkyl peroxy radical, generated by the decomposition of AAPH in aerated solution. This radical was chosen as an example of peroxy radicals, widely present in a lot of real systems. The modified electrode was immersed for 30 min in a 0.133 M AAPH solution kept at 40 °C, and again no effect was observed on the charge transfer of Ru $(NH_3)_6^{3+}/Ru(NH_3)_6^{2+}$ couple.

The superoxide radicals were generated by the autoxidation of pyrogallol [40,41]. The electrode was soaked for 2 h in a 10 mM phosphate buffer (pH 8.0) containing 5 mM pyrogallol. Then it was washed and the voltammetric response recorded. The behavior of the electrode was perfectly insulating, suggesting that the superoxide radical does not interfere with the determination.

Finally, we tested the effect of a strong oxidant on the film. After soaking the electrode in a 0.1 $KMnO_4$ solution the signal of $Ru(NH_3)_6^{3+}/Ru(NH_3)_6^{2+}$ couple was partly restored. In this case, the interference is effective but fortunately strong oxidants are absent in most of real matrices.

3.5. Determination of the activity of different photocatalysts

The modified electrode was used to evaluate the OH radicals produced by five different photocatalysts based on TiO_2 nanoparticles. Two of them were commercial catalysts (Colorobia Spa, Italy) while the other three were prepared from commercial products. The photocatalyst suspensions had different pHs and the nanoparticles were stabilized in different ways. The (%) degradations caused by the irradiation of the photocatalyst suspensions were in the range 0.5–2.5%.

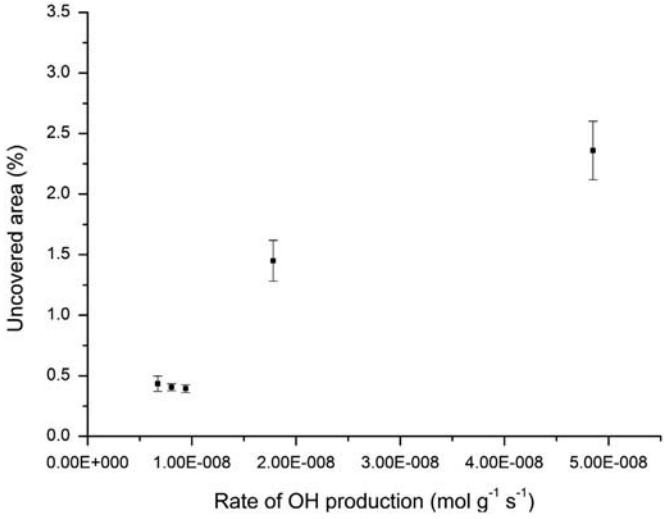

Fig. 6. OH production rates (M min^{-1}) for different TiO_2 photocatalysts, evaluated using SA as OH probe, plotted vs. the % uncovered area determined by CA of the polyphenol-modified GC. The error bars represent the standard deviation of three measurements.

The photocatalytic activity was also studied using the HPLC method which exploits salicylic acid as ·OH trapping agent [42,43]. Eq. (1) was used to estimate the OH radical production by the different photocatalysts. Since the kinetic constant of ·OH reaction with SA is very high (2.0×10^{10} M^{-1} s^{-1}) and there is no other scavenger in the solution, $Km \cdot [\text{matrix}]$ term is negligible. The yield (η) values were estimated for the pHs of the different photocatalyst suspensions and these values agreed with what is reported in the literature [44].

In Fig. 6 the uncovered areas (%) of the polyphenol films were plotted vs. the values of OH production evaluated by the chromatographic method. A good linear correlation between the two sets of data was found being R^2 equal to 0.91. It must be taken into account that the two methods evaluate different physicochemical quantities. The HPLC procedure using SA as an OH

trapping agent quantifies the OH production without considering its consumption; the proposed sensor evaluates the ·OH flux towards the electrode surface, hence all the reactions involving the OH radicals play an important role in the generation of the analytical signal.

4. Conclusion

An insulating film of polyphenol was used as a modifier of GC electrodes to develop a sensor for the indirect determination of the OH radical. The ·OH attack partially removes the polyphenol film from the electrode surface leaving an uncovered area which can be evaluated from the electrochemical signal of the redox probe $Ru(NH_3)_6^{3+}$. The uncovered area percentage was found proportional to the ·OH production suggesting that the sensor can be used for the determination of the OH radicals.

In particular, the observed analytical signal is related to the oxidant capacity of the OH radicals diffusing *towards* a surface. Therefore, the proposed sensor could be useful to make a relative scale of ·OH concentration in similar matrices, as other indirect methods above cited do, with the obvious advantage to avoid a chromatographic or electrophoretic separation.

The alkyl peroxy, superoxide and $ABTS^{\cdot+}$ radicals were studied to check their possible interference on the ·OH determination. They displayed none. $KMnO_4$, also tested as possible interferent, led to an increase of the analytical signal. Fortunately, strong oxidants like permanganate are absent in most of the matrices of interest.

The proposed sensor was used to evaluate the OH radical produced by five different kinds of photocatalysts, based on TiO_2 nanoparticles. The obtained results were in agreement with those estimated by means of a more traditional chromatographic method supporting the feasibility of the proposed approach. In our opinion, the device here described can be considered a good tool for a rapid detection of ·OH level in various matrices or for other purposes as, for instance, the evaluation of the antioxidant capacity of a series of compounds. Moreover, it is cheap and easy to prepare.

The analytical performance of the polyphenol-modified GC is strictly connected to the ability to prepare repeatable films, since the device is disposable.

Appendix A. Supporting information

Supplementary data associated with this article can be found in the online version at http://dx.doi.org/10.1016/j.talanta.2013.06.043.

References

[1] S. Cuzzocrea, R.J. Ruiter, Eur. J. Pharmacol. 426 (2001) 1–10.
[2] H. Yahamoto, T. Watanabe, H. Mizuno, K. Endo, T. Hosowaka, A. Kazusaka, R. Gooneratne, S. Fujita, Free Radical Biol. Med. 30 (2001) 547–554.
[3] S. Turnbull, B.J. Tabner, D.R. Brown, D. Allsop, Biochemistry—US 42 (2003) 7675–7681.
[4] B.J. Tabner, S. Turnbull, O.M.A. El-Agnaf, D. Allsop, Free Radical Biol. Med. 32 (2002) 1076–1083.
[5] C. Schöneich, D. Pogocki, G.L. Hug, K. Bobrowski, J. Am. Chem. Soc. 125 (2003) 13700–13713.
[6] D.P. Naughton, J. Knappitt, K. Fairburn, F. Gaffney, D.R. Blake, M. Grootveld, FEBS Lett. 361 (1995) 167–172.
[7] T. Yamamoto, S. Yuki, T. Watanabe, M. Mitsuka, K.I. Saito, K. Kogure, Brain Res. 762 (1997) 240–242.
[8] H. Negeshi, K. Ikeda, Y. Nara, Y. Yamori, Neurosci. Lett. 306 (2001) 206–208.
[9] K. Ito, S. Inoue, Y. Hiraku, S. Kawanishi, Mutat. Res.—Gen. Toxicol. Environ. 585 (2005) 60–70.
[10] J.J. Pignatello, Environ. Sci. Technol. 26 (1992) 944–951.
[11] J. Hoigne, H. Bader, Water Res. 10 (1976) 377–386.
[12] G.E. Orzechowska, E.J. Poziomek, V.F. Hodge, W.H. Engelmann, Environ. Sci. Technol. 29 (1995) 1373–1379.
[13] J.J. Pignatello, G. Chapa, Environ. Sci. Technol. 13 (1994) 423–427.
[14] G.R. Peylon, W.H. Glaze, Environ. Sci. Technol. 22 (1988) 761–767.
[15] T. Mill, The Handbook of Environmental Chemistry. Part A, in: in: O. Hutzinger (Ed.), Springer-Verlag, Berlin, 1980, pp. 77–105.
[16] J. Seinfeld, S. Pandis, Atmospheric Chemistry and Physics, Wiley, Hoboken, 2006.
[17] Y.-L. Hu, Y. Lu, G.-J. Zhou, X.-H. Xia, Talanta 74 (2008) 760–765.
[18] S. Kataoka, H. Yasui, M. Hiromura, H. Sakurai, Life Sci. 77 (2005) 2814–2829.
[19] H.H. Shi, X.R. Wang, Y. Luo, Y. Su, Aquat. Toxicol. 74 (2005) 365–371.
[20] S.Y. Ai, Q.J. Wang, H. Li, L.T. Jin, J. Electroanal. Chem. 578 (2005) 223–229.
[21] F. Blandini, E. Martignoni, R. Ricotti, F. di Jeso, G. Nappi, J. Chromatogr. B 732 (1999) 213–220.
[22] Y.H. Cao, Q.C. Chu, J.N. Ye, Anal. Bioanal. Chem. 376 (2003) 691–695.
[23] B. Pal, P.A. Ariya, Environ. Sci. Technol. 38 (2004) 5555–5566.
[24] C.W. Lau, X.J. Qin, J.Y. Liang, J.Z. Lu, Anal. Chim. Acta 514 (2004) 45–49.
[25] S.A.J. Coolen, F.A. Huf, J.C. Reijenga, J. Chromatogr. B 717 (1998) 119–124.
[26] C. von Sonntag, Free-Radical-Induced DNA Damage and Its Repair, SpringerHeildenberg, 2006.
[27] L.D. Mello, S. Hernadez, G. Marrazza, M. Mascini, L.T. Kubota, Biosens. Bioelectron. 21 (2006) 1374–1382.
[28] F. Scholtz, G. Lopez de Lara Gonzàlez, L. Machado de Carvalho, M. Hingelmann, K.Z. Brainina, H. Kahrlet, R. Smail Jack, D Troug Minh, Angew. Chem. Int. Ed 46 (2007) 8079–8081.
[29] L. Wu, Y. Yang, H. Zhang, G. Zhu, X. Zhang, J. Chen, Anal. Chim. Acta 756 (2012) 1–6.
[30] A.J. Bard, L.R. Faulkner, Electrochemical Methods: Fundamentals and Applications, second ed., Wiley, New York, 2000.
[31] T. Gueshi, K. Tokuda, M. Matsuda, J. Electroanal. Chem. 89 (1978) 247–260.
[32] M. Gattrell, D.W. Kirk, J. Electrochem. Soc. 139 (1992) 2736–2744.
[33] M. Gattrel, D.W. Kirk, J. Electrochem. Soc. 140 (1993) 903–911.
[34] P. Garces, R. Lapuente, L.G. Andion, F. Cases, E. Morralon, J.L. Vasquez, Polym. J. 32 (2000) 623–628.
[35] H.B. Dunford, Coordin. Chem. Rev.233 and 234 (2002) 311–318.
[36] E. Neyens, J. Baeyens, J. Hazard. Mater. B 98 (2003) 33–50.
[37] C.L. Lin, N.K. Rohatgi, W.B. DeMore, Geophys. Res. Lett. 5 (1978) 113–115.
[38] J.P. Hunt, H. Taube, J. Am. Chem. Soc. 74 (1952) 5999–6002.
[39] H. Yamaguchi, Y. Uchihori, N. Yasuda, M. Takada, H.J. Kitsmura, Radiat. Res. 46 (2005) 333–341.
[40] X. Li, J. Agr. Food Chem. 60 (2012) 6418–6424.
[41] M.R. Miller, S.J. Bortthwick, C.A. Shaw, S.G. McLean, D. McClure, N.L. Mills, R. Duffin, K. Donaldson, I.A. Megson, P.W.F. Hadoke, D.E. Newby, Enviromen. Health Perspect. 117 (2009) 611–616.
[42] N. Shimizu, C. Ogino, M.F. Dadjour, K. Nihomiya, A. Fuijhira, K. Sakiyama, Ultrason. Sonochem. 15 (2008) 988–994.
[43] T-.C. Cheng, K.-S. Yao, Y.-H. Hsich, L.-L. Hsich, C.Y. Cheng, Mater. Design 31 (2010) 1749–1751.
[44] R.A. Salmon, C.L. Schiller, G.W. Harris, J. Atmos. Chem. 48 (2004) 81–104.